Available online at www.sciencedirect.com
SCIENCE DIRECT®
International Journal of Solids and Structures 42 (2005) 1173–1186
INTERNATIONAL JOURNAL OF SOLIDS and STRUCTURES
www.elsevier.com/locate/ijsolstr

Large deflections of deep orthotropic spherical shells under radial concentrated load: asymptotic solution

Alexander Yu. Evkin *

Department of Mathematics, King Fahd University of Petroleum and Minerals, Hail Community College, P.O. Box 2440, Hail, Saudi Arabia

Received 24 December 2003; received in revised form 7 July 2004
Available online 2 September 2004

Abstract

Nonlinear behavior of deep orthotropic spherical shells under inward radial concentrated load is studied. The singular perturbation method is developed and applied to Reissner's equations describing axially symmetric large deflections of thin shells of revolution. A small parameter proportional to the ratio of shell thickness to the sphere radius is used. The simple asymptotic formulas describing load–deflection diagrams, maximum bending and membrane stresses of the structure are derived. The influence of boundary conditions on the behavior of the shell by large deflections is considered. Obtained asymptotic solution is in close agreement with the experimental and numerical results and has the same accuracy (in the asymptotic meaning) as the given equations of nonlinear theory of thin shells.

Keywords: Orthotropic spherical shell; Large deflections; Asymptotic analysis; Concentrated load

1. Introduction

A number of experimental and numerical solutions (Ashwell, 1959; Evan-Iwanowski et al., 1962; Mescall, 1965; Bushnell, 1967; Fitch, 1968; Penning and Thurston, 1965; Penning, 1966) of the classical problem of thin isotropic spherical shell under inward point load have shown the significant difference in the behavior and stress equilibrium state of the structure by small and large deflections. When the

* Tel.: +966 531 2500; fax: +966 531 0500.
E-mail address: alexyevkin@hotmail.com

0020-7683/$ - see front matter © 2004 Elsevier Ltd. All rights reserved.
doi:10.1016/j.ijsolstr.2004.07.002

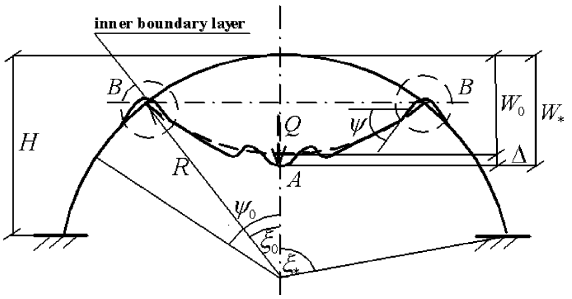

Fig. 1. Large deflections of deep spherical shell under concentrated load.

deflections do not exceed the thickness of the shell, deformations of the shell are localized near the load point and displacements die away rapidly with the distance from the load. In this case the linear shallow (technical) shell theory can be applied for the practical purposes. In contrast, by large deflections the middle surface of the deformed shell is close to the spherical dimple of curvature equal to the initial shell curvature, but of opposite sign (Fig. 1). This shape of the shell (reflected segment with respect to the plane perpendicular to the symmetry axes) is isometric to the initial sphere, which means that the middle surface is free of membrane deformations and only bending deformations exist in the shell. There is also a narrow region (inner boundary layer B in Fig. 1) of strong both bending and membrane deformations and still small displacements. The base radius of the dimple increases, when the load rises. Several authors (Ashwell, 1959; Ranjan and Steele, 1977) used these observations as assumptions to obtain the analytical solutions of the problem both for shallow and deep but isotropic spherical shells. They constructed solution in the region B, connecting both parts of deformed structure (initial sphere and its inverted part), and then applied variation method minimizing the total potential energy with respect to the base radius of the dimple. The boundary conditions were ignored in these investigations, which is correct when the region B is far enough from the edge of the shell.

The present investigation is based on the asymptotic analysis (Evkin and Kalamkarov, 2001a,b) of Reissner's equations (Reissner, 1969, 1972) describing axially symmetric deformations of thin elastic deep shells of revolution by large deflections and rotation angles. A small parameter proportional to the ratio of the shell thickness to its radius was used in the paper. This parameter appeared at the highest order derivatives of the initial equations, therefore a singular perturbation analysis was used to obtain the solution, which contains two parts: smooth solution, corresponding to inverted segment of the sphere plus its initial part, and fast changing solution (inner boundary layer B in Fig. 1), connecting these parts of smooth solutions. As a result of asymptotic analysis, the main assumptions of previous investigations were obtained. Furthermore, it was shown that the accuracy of asymptotic solution coincides with the accuracy of the given Reissner's equations of thin shell theory. In present paper we intend to apply the asymptotic approach and equations (Evkin and Kalamkarov, 2001a,b) to the case of deep orthotropic spherical shell under concentrated load and also to expand and verify the analytical solution (Ranjan and Steele, 1977) obtained for isotropic shells. We also are going to investigate the stress states of shells as well as influence of boundary conditions on the behavior of orthotropic spherical shells and provide simple asymptotic formulas, which would be useful for practical purposes. It is worth to mention, that although the numerical methods (Mescall, 1965; Penning and Thurston, 1965; Bushnell, 1967; Fitch, 1968) were successful, they require sophisticated techniques and tools for solving such problems as analysis of thin shells by large deflections because of singularity of initial nonlinear differential equations. The difficulties of obtaining numerical solutions increase for larger deflections and thinner shells, but, in contrast, the suggested asymptotic method is more efficient in these cases.

2. Asymptotic equations and solution

We apply the asymptotic equations (Evkin and Kalamkarov, 2001a,b) obtained for rather general case of large axially symmetric deflections of composite shells of revolution simplifying them for the case of orthotropic spherical shell. We use formulas, linking generalized internal loads and axially symmetric deformations, in the form, corresponding to orthotropic shell symmetric with respect to its middle surface

$$N_i = B_{ij}\varepsilon_j, \quad M_i = D_{ij}\chi_j \ \ (i,j=1,2) \tag{2.1}$$

where ε_1 and ε_2 are the deformations of midsurface element in the meridional and circumferential directions, χ_1 and χ_2 are corresponding curvature variations, N_1 and M_1 are the stress resultant and bending moment that arise in a unit area perpendicular to the meridian, N_2 and M_2 are the corresponding internal force and moment that act on a unit area in the plane of the meridian. For the particular case of isotropic shell we have the following formulas for the elements of stiffness matrices (2.1):

$$B_{11} = B_{22} = \frac{Eh}{1-\nu^2}, \quad D_{11} = D_{22} = \frac{Eh^3}{12(1-\nu^2)}$$

where h is the shell thickness, E and ν are the elasticity modulus and Poisson's ratio of the material.

For the asymptotic analysis we introduce a small parameter, which is defined as

$$\varepsilon^2 = \frac{h}{R}\sqrt{\frac{D_{11}}{a_* B_{22} h^2}} \tag{2.2}$$

where R is radius of sphere, $a_* = 1 - \frac{B_{12}^2}{B_{11}B_{22}}$.

For an isotropic spherical shell we have parameter

$$\varepsilon^2 = \frac{h}{R\sqrt{12a_*}} \tag{2.3}$$

where $a_* = 1-\nu^2$. This parameter is really small and well known in the linear theory of thin shells. Apparently, it will be also small for orthotropic shells if

$$\frac{D_{11}}{a_* B_{22} h^2} \sim O(1) \tag{2.4}$$

We use two terms of asymptotic expansion

$$\overline{Q} = \overline{Q}_0 + \varepsilon\overline{Q}_1 \tag{2.5}$$

of the concentrated load Q introducing dimensionless load parameter

$$\overline{Q} = \frac{Q}{4\pi\sqrt{a_* D_{11} B_{22}}} \tag{2.6}$$

According to Evkin and Kalamkarov (2001a,b) we will distinguish two quite different cases of asymptotic analysis: when the inner boundary layer is far from the edge of the shell and we can neglect the influence of edge conditions, and when the edge of the shell is interfering with the inner boundary layer. For the first case we have the following asymptotic equations:

$$\frac{\mathrm{d}^2\psi}{\mathrm{d}\xi^2} = \overline{U}\sin\psi \tag{2.7}$$

$$\frac{\mathrm{d}^2\overline{U}}{\mathrm{d}\xi^2} = \frac{\cos\psi - \cos\xi_0}{\sin^2\xi_0} \tag{2.8}$$

with boundary conditions

$$\overline{U} = 0, \quad \psi = \pm\xi_0 \quad \text{as} \quad \xi \to \pm\infty \tag{2.9}$$

where $\xi = \frac{\psi_0 - \xi_0}{\varepsilon}$, ξ_0 is the angle defining the location of the inner boundary layer or the base radius of dimple (Fig. 1), ψ_0 is the angle coordinate of the current shell point, ψ_0 and ψ are the angles of inclination of the tangent to the meridian before and after shell deformation (Fig. 1). Boundary conditions (2.9) correspond to two parts of smooth solution: initial sphere ($\psi = \xi_0$ at $\psi_0 = \xi_0$) and inverted part of the sphere segment ($\psi = -\xi_0$ at $\psi_0 = \xi_0$). Boundary layer functions $\psi(\xi)$ and $\overline{U}(\xi)$, connecting these two solutions and describing stress state of the shell in the region B, are functions giving stress resultants and bending moments in the following form:

$$N_2 = \frac{D_{11}^{1/4}(a_* B_{22})^{3/4}}{\sqrt{R}} \sin\xi_0 \overline{U}'(\xi), \quad N_1 = 0 \tag{2.10}$$

$$M_1 = \frac{D_{11}}{\varepsilon R}\psi'(\xi), \quad M_2 = \frac{D_{21}}{D_{11}} M_1 \tag{2.11}$$

It is significant that the boundary value problem (2.7)–(2.9) depends only on one parameter ξ_0 defining the position of the inner boundary layer, but does not depend on structure properties and on the type of external load. Having the solution of this problem, it is easy to obtain the asymptotic formula for deformation energy of the shell, which is concentrated at inner boundary layer and therefore can be expressed by functions $\psi(\xi)$ and $\overline{U}(\xi)$ in the form (Evkin and Kalamkarov, 2001a,b)

$$W(\xi_0) = a_* \pi B_{22} R^2 \xi_0^2 \sin\xi_0 \varepsilon^3 J \tag{2.12}$$

where

$$J = \int_{-\infty}^{+\infty} [f^2 + (\varphi')^2]\,\mathrm{d}\xi \tag{2.13}$$

and

$$f = \frac{\sin\xi_0}{\xi_0}\overline{U}', \quad \varphi = \frac{\psi}{\xi_0} \tag{2.14}$$

Work of constant concentrated load, applied at the apex of the spherical shell, could be easily represented as

$$A_1 = Q W_0(\xi_0), \quad W_0(\xi_0) = 2R(1 - \cos\xi_0) \tag{2.15}$$

where W_0 is the deflection amplitude of the shell.

Both work of load and deformation energy of the shell depend only on one parameter ξ_0. Minimizing the total potential energy with respect to this parameter we have the following condition:

$$\frac{\partial W}{\partial \xi_0} = \frac{\partial A_1}{\partial \xi_0} \tag{2.16}$$

which yields the asymptotic formula

$$\overline{Q}_1 = \frac{\xi_0}{8\sin\xi_0}\left(2J\sin\xi_0 + \xi_0 J\cos\xi_0 + \frac{\mathrm{d}J}{\mathrm{d}\xi_0}\xi_0\sin\xi_0\right), \quad \overline{Q}_0 = 0 \tag{2.17}$$

where

$$Q = 4\pi\varepsilon\overline{Q}_1\sqrt{a_* D_{11} B_{22}} \tag{2.18}$$

The boundary value problem (2.8) and (2.9) was solved in (Evkin and Korovaitsev, 1992) numerically. The obtained result is represented by expression

$$J(\xi_0) = J_0 + 0.116\xi_0^2 \tag{2.19}$$

where $J = J_0 = 2.23$ is part of the solution corresponding to shallow shells.

For bending moments and stress resultants we have the following asymptotic formulas:

$$M_1 = \frac{D_{11}\xi_0}{\varepsilon R}\varphi'(\xi), \quad M_2 = \frac{D_{12}}{D_{11}}M_1, \quad N_2 = a_* B_{22}\varepsilon\xi_0 f(\xi), \quad N_1 = 0 \tag{2.20}$$

For estimation of the stress state of structure we have useful formulas for maximum values of internal forces

$$\max|M_1| = \frac{D_{11}\xi_0}{\varepsilon R}\max|\varphi'|, \quad \max|M_2| = \frac{D_{12}}{D_{11}}\max|M_1| \tag{2.21}$$

$$\max|N_2| = a_* B_{22}\varepsilon\xi_0 \max|f|, \quad |N_1| \ll |N_2| \tag{2.22}$$

where

$$\max|f| = 0.4 + 0.005\xi_0^2, \quad \max|\varphi'| = 0.95 + 0.08\xi_0^2 \tag{2.23}$$

Now we are in the position ready to analyze obtained asymptotic formulas and represent them in the final form convenient for applications in the practical engineering. For this purpose we use approximations

$$\sin\xi_0 \approx \xi_0, \quad \cos\xi_0 \approx 1 - \frac{\xi_0^2}{2}$$

corresponding to shallow shells and obtain the following expressions:

$$\xi_0 = \sqrt{\frac{W_0}{R}}, \quad J \approx J_0 = 2.23$$

which yield

$$\overline{Q}_1 = \frac{3J_0\xi_0}{8} = \frac{3J_0}{8}\sqrt{\frac{W_0}{R}} \tag{2.24}$$

Comparing both asymptotic solutions (2.17) and (2.24) for deep and shallow shells, we derived that there is no difference between these solutions if $\xi_0 \leqslant 1.3$. Thus, formula (2.24) can be expanded to such deep spherical shells under concentrated load. The maximum difference occurs at $\xi_0 = \pi/2$ (semi sphere), when formula (2.24) gives the value 7.5% greater then more accurate solution (2.17) corresponding to deep shells. But, according to (2.23), the distinction in formulas for bending moment can reach 25% at $\xi_0 = \pi/2$.

Formula (2.24) can be written in the form

$$\frac{W_0}{R} = \left(\frac{8\overline{Q}_1}{3J_0}\right)^2 \tag{2.25}$$

This asymptotic formula is valid only for large deflections. To expand it for small deflections we will follow the idea described in (Ranjan and Steele, 1977). In this paper the linear solution of the spherical shell under concentrated load are considered. The linear solution is valid for small deflections and can be written in the following form:

$$\frac{\Delta}{R} = \frac{\pi\varepsilon\overline{Q}_1}{2} \tag{2.26}$$

Because the corresponding stress state is localized near the load point and the linear solution does not depend on how the load is applied (inward or outward the shell), we can calculate the total deflection amplitude as the sum of two terms (Fig. 1)

$$\frac{W_*}{R} = \frac{W_0}{R} + \frac{\Delta}{R} \tag{2.27}$$

The obtained expression can be considered as a joint solution valid both for small and large deflections. In fact, the solution is valid for large deflections as an asymptotic one, but it is also true for small deflections, because its first term can be neglected as load parameter tends to 0 and we obtain formula (2.26) in this case.

For further analysis we represent formula (2.27) in the form

$$\frac{W_*}{h} = \frac{W_0}{h} + \frac{\Delta}{h} \tag{2.28}$$

$$\frac{W_0}{h} = \left(\frac{8\,\widehat{Q}}{3J_0}\right)^2 \tag{2.29}$$

$$\frac{\Delta}{h} = \frac{\pi}{2}\varepsilon\sqrt{\frac{R}{h}}\widehat{Q} \tag{2.30}$$

where $\widehat{Q} = \overline{Q}_1\sqrt{\frac{R}{h}}$.

The obtained formula (2.28) coincides with formula (53) from (Ranjan and Steele, 1977), if

$$\widehat{Q} = \frac{1}{4\pi}[12(1-\nu^2)]^{3/4}P', \quad P' = \frac{QR}{Eh^3}, \quad J_0 = 8\sqrt{2}/5 \approx 2.26$$

Thus, result (2.28) could be considered as validation (in asymptotic meaning) of solution obtained in (Ranjan and Steele, 1977) for isotropic shells and as its expansion to the case of orthotropic structures. Note, that for isotropic shells the coefficient in (2.30) is $\varepsilon\sqrt{\frac{R}{h}} = \frac{1}{[12(1-\nu^2)]^{1/4}}$.

Two components of solution (2.28) are shown in Fig. 2. Curve 1 corresponds to asymptotic solution by large deflections (2.29), curve 2 corresponds to the linear solution (2.30). Joint solution (2.28) (curve 3) is

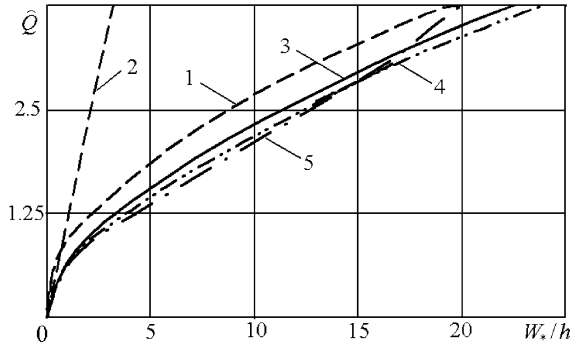

Fig. 2. Load-deflection diagram of orthotropic spherical shell.

very close to both experimental (Penning and Thurston, 1965) and numerical (Fitch, 1968) results obtained for the case of isotropic shells and represented in Fig. 2 by curves 4 and 5 respectively. Thus, formulas (2.28)–(2.30) could be recommended for engineering design as well as for investigation of axially symmetric deformations of orthotropic spherical shell structures under concentrated load. In case of quite deep shells formulas (2.15), (2.17)–(2.19) should be used instead of (2.29).

According to experimental results (Penning and Thurston, 1965), the deformation of thin isotropic spherical shell becomes asymmetric, when deflection amplitude reaches about 20–30 times the shell thickness. The estimation of a limit of axially symmetric theory of orthotropic spherical shell could be found in (Evkin and Dubichev, 1995). In the present paper we will mention only the final asymptotic formula obtained for the first point of bifurcation of equilibrium shape of shell into non-axisymmetric (trilobate) configuration. It occurs at the deflection amplitude

$$W_0 = \frac{81}{J_0^2}\left(\frac{D_{11}}{a_* B_{22}}\right)^{1/2}\left(1+\frac{D_{22}}{D_{11}}+\frac{2(T+D_{12})}{3D_{11}}\right)^2$$

Here T is the torsion stiffness, which should be taken into account while considering non-symmetric deformation of the shell. Interestingly, the obtained result does not depend on the type of load. It is valid for concentrated load as well as for uniform external pressure. In the particular case of isotropic shell we have

$$W_0 = \frac{96\sqrt{3}h}{J_0^2\sqrt{1-\nu^2}}$$

Approximately $W_0 \approx 33h$ in this case. In the experimental studies (Penning and Thurston, 1965) the non-symmetric components of the equilibrium configuration were observed, when the deflection amplitude was smaller (about 20–30 times the shell thickness). This difference could be the consequence of assumptions of the applied asymptotic method as well as influence of shell imperfections. On the other hand, the case when the inner boundary layer is located far from the edge of the shell is considered in the theory, but the support of the shell on a non-deformable rim creates an additional obstacle to the emergence of non-axisymmetric deflection components (Evkin and Dubichev, 1995).

Another very important practical task is the evaluation of stresses arising in the shell. First of all, let us analyze the distribution of the bending and membrane stresses along the meridian. It depends on functions $\varphi'(\xi)$ and $f(\xi)$, which were obtained by solving the boundary value problem (2.7)–(2.9) and are shown in Fig. 3 for the case of shallow shell. Function $f(\xi)$ is odd one, but function $\varphi'(\xi)$ is even. It is important to note, that the maximums of bending moments ($\max|\varphi'|$) occur at $\xi = 0$, when the membrane stress resultants are equal to 0 ($f = 0$). For the bending stresses one can derive the following formulas:

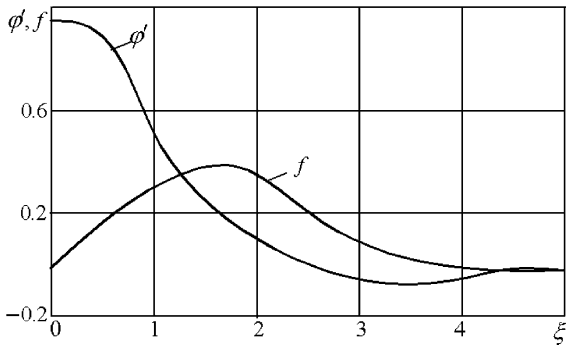

Fig. 3. Distribution of stresses in the spherical shell.

$$\max|\sigma_1^{\mathrm{b}}| = \frac{6\max|M_1|}{h^2} = \frac{6D_{11}\xi_0}{\varepsilon R h^2}\max|\varphi'| \tag{2.31}$$

$$\max|\sigma_2^{\mathrm{b}}| = \frac{6\max|M_2|}{h^2} = \frac{6D_{12}\xi_0}{\varepsilon R h^2}\max|\varphi'| \tag{2.32}$$

For membrane stresses we have

$$\max|\sigma_2^{m}| = a_* B_{22}\varepsilon\xi_0 \max|f|/h \tag{2.33}$$

Here $\max|\varphi'|$ and $\max|f|$ should be calculated using (2.23). For the comparison of bending and membrane stresses we consider their ratio

$$\frac{\max|\sigma_1^{\mathrm{b}}|}{\max|\sigma_2^{m}|} = \frac{6h\varepsilon^2}{R}\frac{\max|\varphi'|}{\max|f|}$$

which for isotropic sphere yields the following:

$$\frac{\max|\sigma_1^{\mathrm{b}}|}{\max|\sigma_2^{m}|} = \sqrt{\frac{3}{1-\nu^2}}\frac{\max|\varphi'|}{\max|f|} > 4.1$$

One can conclude now that formulas (2.31) and (2.32) for bending stresses are of the main importance in analysis of the strength of the structure and membrane stresses can be neglected.

3. The influence of boundary conditions on the behavior and stress state of the shell

According to Evkin and Kalamkarov (2001a,b), the load increases, when the inner boundary layer approaches the edge of the shell. In this case the first term of the asymptotic expansion $\overline{Q} = \overline{Q}_0 + \varepsilon\overline{Q}_1$ is not equal to 0 and the full asymptotic shell equations instead of (2.7) and (2.8) have the following form:

$$\frac{\mathrm{d}^2\psi}{\mathrm{d}\xi^2} = \overline{U}\sin\psi + 2q_0\xi_*\cos\psi \tag{3.1}$$

$$\frac{\mathrm{d}^2\overline{U}}{\mathrm{d}\xi^2} = \frac{\cos\psi - \cos\xi_*}{\sin^2\xi_*} \tag{3.2}$$

where angle ξ_* defines the location of the edge of the shell (Fig. 1) and the load parameter q_0 is given as

$$q_0 = \frac{\overline{Q}_0}{\xi_*\sin\xi_*} = \frac{Q}{4\pi\xi_*\sin\xi_*\sqrt{a_* D_{11}B_{22}}} \tag{3.3}$$

Eqs. (3.1) and (3.2) describe the stress state of the shell in the inner boundary layer, which is now close to the shell edge.

In order to complement the specification of the boundary value problem we introduce the parameter t defining the location of the shell edge relatively to the inner boundary layer

$$t = (\xi_* - \xi_0)/\varepsilon \tag{3.4}$$

The boundary conditions can be represented in the following form (at $\xi = t$):

$$\psi = \xi_*, \quad \overline{U}' = 0 \tag{3.5}$$

$$\psi = \xi_*, \quad \overline{U} = 0 \tag{3.6}$$

$$\psi' = 0, \quad \overline{U}' = 0 \tag{3.7}$$

The first condition corresponds to the shell clamped along circumference $\psi_0 = \xi_*$, the second corresponds to an edge resting on a frictionless surface, and the last one corresponds to the simply supported edge. Besides, we impose conditions of transferring of boundary layer functions to solution corresponding to the inverted segment

$$\psi = -\xi_*, \quad \overline{U} = 2q_0\xi_* \cot\xi_* \text{ as } \xi \to -\infty \tag{3.8}$$

We simplify the obtained boundary value problem by introducing approximations

$$\sin x \approx x, \quad \cos x \approx 1 - 0.5x^2, \quad \cot x \approx x$$

which correspond to the technical shallow shell theory containing only quadratic nonlinear terms. After change of variables

$$\overline{U} = 2\varphi_0, \quad \psi = \xi_*(1 - 2w_0) \tag{3.9}$$

we come to the equations

$$w_0'' + \varphi_0(1 - w_0) + q_0 = 0 \tag{3.10}$$

$$\varphi_0'' - w_0(1 - w_0) = 0 \tag{3.11}$$

with one of the following boundary conditions (at $\xi = t$)

$$w_0 = 0, \quad \varphi' = 0 \text{ (clamped edge)} \tag{3.12}$$

$$w_0 = 0, \quad \varphi = 0 \text{ (edge on a frictionless surface)} \tag{3.13}$$

$$w_0' = 0, \quad \varphi' = 0 \text{ (simply supported edge)} \tag{3.14}$$

and also

$$w_0 = 1, \quad \varphi_0 = q_0 \text{ at } \xi \to -\infty \tag{3.15}$$

instead of (3.8).

Formulas (2.20) for bending moments and stress resultants take now the form

$$M_1 = -w_0'(t)\frac{2D_{11}\sqrt{W_0}}{\varepsilon R^{3/2}}, \quad M_2 = M_1\frac{D_{12}}{D_{11}} \tag{3.16}$$

$$N_2 = 2a_*B_{22}\varepsilon\sqrt{\frac{W_0}{R}}\varphi_0'(t), \quad N_1 = 0 \tag{3.17}$$

where W_0 is the deflection amplitude, which could be defined from the expression $\xi_0 = \sqrt{\frac{W_0}{R}}$.

The boundary value problem (3.10)–(3.15) coincides with that obtained in (Evkin and Kalamkarov, 2001a,b) for the case of external uniform pressure q with the following asymptotic expansion

$$\bar{q} = \bar{q}_0 + \varepsilon\bar{q}_1, \quad \bar{q} = q/q_*, \quad q_* = \frac{4}{R^2}\sqrt{a_*D_{11}B_{22}}$$

therefore we can use directly the numerical solution obtained in this paper. It is shown in Figs. 4 and 5. The first one exhibits the dependence of the load parameter q_0, when the inner boundary layer approaches the edge of the shell ($\xi_0 \to \xi_*$ or $t \to 0$) for different types of boundary conditions. The similar curves are displayed in Fig. 5, where maximum of function $|w_0'(t)|$ is shown. This maximum corresponds to the maximum bending stresses according to (3.16). We do not consider membrane stresses here (function $|\varphi_0'(t)|$), because

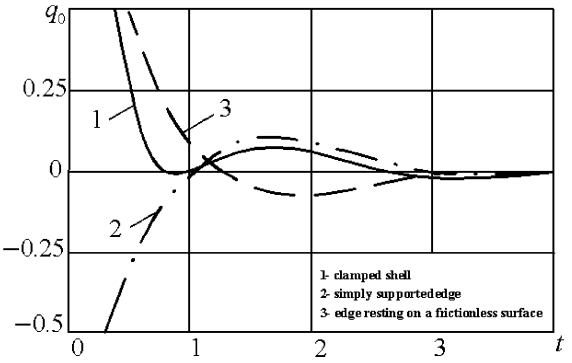

Fig. 4. Load parameter of inverted shell for different boundary conditions.

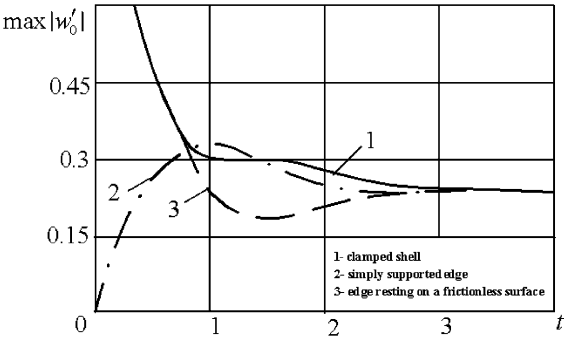

Fig. 5. Bending stress parameter of inverted spherical shell.

they are much smaller compared to bending ones for any type of boundary conditions. In case of shallow spherical shell we have $\xi_* = \sqrt{\frac{2H}{R}}$ and $\xi_0 = \sqrt{\frac{W_0}{R}}$, therefore

$$t = \frac{\sqrt{2H} - \sqrt{W_0}}{\varepsilon\sqrt{R}} \tag{3.18}$$

Parameter $t = 0$, if the deflection amplitude of shell reaches $2H$, where H is the rise of the cap.

The behavior of shell with different boundary conditions changes when t tends to 0 (fully inverted shell). The load dramatically increases for the case of clamped shell while it changes from positive to negative for the simply supported shell. Load parameter $q_0 \approx 0$ for relatively large t ($t \geqslant 4$ for the clamped shell and $t \geqslant 3$ for the simply supported one), which corresponds to the location of boundary layer sufficiently far from the edge of the shell. In this case $\overline{Q}_0 = 0$ in the expansion (2.5) and formulas of the previous section can be used. But, when the inner boundary layer interferes with the edge of the shell, two terms of expansion (2.5) must be used and the final formula for load deflection relation of shallow orthotropic spherical shell can be represented in the following form:

$$Q = 4\pi\sqrt{a_* D_{11} B_{22}}\left(\frac{2H}{R}q_0(t) + \frac{3J_0\varepsilon}{8}\sqrt{\frac{W_0}{R}}\right) \tag{3.19}$$

where $J_0 = 2.23$ and function $q_0(t)$ could be derived from Fig. 4. For example, in the case of clamped shell (curve 1) this function can be approximated as the following piecewise function:

$$q_0(t) = \begin{cases} 0.5\mathrm{e}^{(0.39-t)}\dfrac{\cos^2 2t}{\cos^2 0.78} & \text{if } 0 < t \leqslant 0.78 \\ 0.0335(1-\cos(3.41(t-0.75))) & \text{if } 0.78 < t \leqslant 1.7 \\ \dfrac{1.34\cos(1.57(t-1.7))}{\mathrm{e}^{1.1(t-1.7)}+\mathrm{e}^{-1.1(t-1.7)}} & \text{if } t \geqslant 1.7 \end{cases} \tag{3.20}$$

The load–deflection diagrams for clamped spherical shells of radius $R = 0.9$ are shown in Fig. 6. Curves 1 and 2 are sketched using formulas (3.19) and (3.20) for two different caps. First one has the rise $H = 0.9$ (semi sphere). The rise of the second one $H = 0.43$. In both cases isotropic shells with modulus of elasticity of material $E = 258{,}000$, Poisson's ratio $v = 0.5$ and thickness of the shell $h = 0.01$ were considered. Corresponding numerical results obtained by applying finite element method are shown by circles and crosses. The whole structure was divided in 36 parts in circumferential direction and only one part with appropriate axial symmetry constraints was retrieved for finite element analysis. The semi spherical shell was meshed in meridian direction to 37 quadrilateral nonlinear shell elements plus one triangular element at the apex of sphere. Then 37 quadrilateral elements were divided in two parts in circumferential direction with constraints of axial symmetry, and we had eventually 75 nonlinear shell elements. In case of spherical shell with the rise $H = 0.43$ we had 47 elements in total. To solve simultaneous nonlinear algebraic equations of finite element method, the Newton–Raphson iterating schema was applied. There is good agreement between both numerical and asymptotic solutions exhibited in Fig. 6. The result of calculation without boundary effect, when in formula (3.19) $q_0 = 0$, is shown by dashed line.

It is interesting that the behavior of shells became non-monotonic, when the inner boundary layer approached the edge of the shell. For instance, the process of numeric calculation converged to two different solutions shown in Fig. 6 for load value equals to 12.6. The main difference is in the shape of shell near the clamped edge. The snap-through buckling AB occurs when the shell is subject to dead loading. In the case of clamped shell we have the cascade of two snap-through buckling paths: CD and AB. In contrast to numerical finite element method the suggested asymptotic solution allowed to obtain the descending parts of the equilibrium paths in Fig. 6. The descending parts correspond to decreasing load because of influence of the first term $q_0(t)$ in the formula (3.19). For the clamped shell we used approximation (3.20) corresponding to the curve 1 in Fig. 4. To obtain the non-monotonic curve 1 we changed the value of variable t and calculated matching value of load parameter $q_0(t)$ satisfying boundary value problem (3.10)–(3.12) and (3.15).

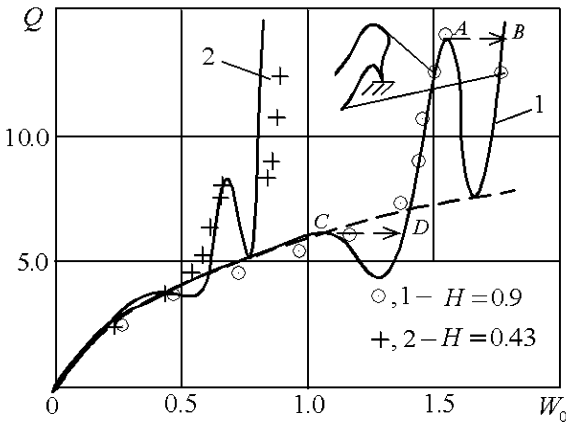

Fig. 6. Load-deflection diagram of clamped spherical shells.

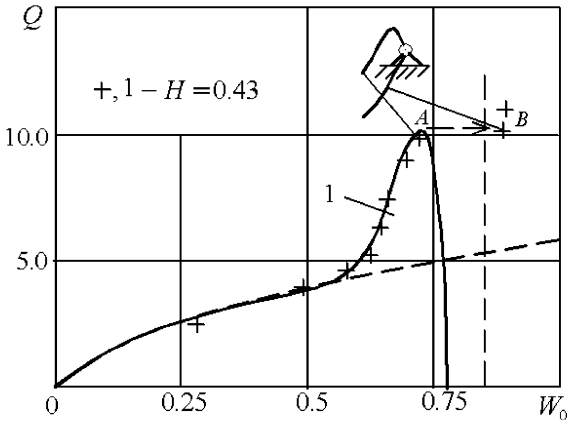

Fig. 7. Load-deflection diagram of simply supported spherical shell.

The behavior of the simply supported spherical shell is shown in Fig. 7. We have in this case one snap-through buckling path AB corresponding to the transformation of the shell equilibrium configuration into fully inverted one. Limit point A corresponds to the buckling load. The dashed vertical line matches the value of deflection amplitude $W_0 = 2H$. For sketching this graph we used curve 2 from Fig. 5 and its approximation by formula

$$q_0(t) = -0.1\sqrt{2}\mathrm{e}^{\pi(0.75-0.5t)}\cos(0.5\pi t), \quad t \geqslant 0.5$$

Let us analyze the graphs of function $\max|w_0'|$ corresponding to maximum bending moments. Fig. 5 shows that bending moments vanish as a simply supported sphere becomes fully inverted ($t \to 0$, $W_0 \to 2H$). Conversely, by inverting clamped shell the bending stresses ($\max|w_0'|$) sharply increase. When the inner boundary layer recedes form the edge (t increases) of the shell, the value of $\max|w_0'|$ tends to the constant equals to 0.475, which corresponds to $\max|\varphi'| = 0.95$ in formula (2.23). It should be noted, that considered function describes only additional boundary layer stresses. The membrane and bending stresses in the main inverted part of the shell could be easily calculated, but they are asymptotically small for shells with large deflections.

The final formulas for maximum bending stresses of orthotropic shallow spherical shell could be represented in the form

$$\max|\sigma_1^{\mathrm{b}}| = \max|w_0'|\frac{12D_{11}\sqrt{W_0}}{\varepsilon h^2 R^{3/2}}, \quad \max|\sigma_2^{\mathrm{b}}| = \max|w_0'|\frac{12D_{12}\sqrt{W_0}}{\varepsilon h^2 R^{3/2}} \tag{3.21}$$

where expression for function $\max|w_0'|$ could be derived from graphs in Fig. 5. For example, in case of clamped shell we obtain approximately

$$\max|w_0'| = \begin{cases} 0.3 + 0.6\mathrm{e}^{(0.35-t)}\dfrac{\cos^2 1.31t}{\cos^2 0.459} & \text{if } 0 < t \leqslant 1.1 \\ 0.3 & \text{if } 1.1 \leqslant t \leqslant 1.6 \\ 0.237 + 0.0313(1+\cos(2.24t - 3.59)) & \text{if } 1.6 < t \leqslant 3 \\ 0.237 & \text{if } t \geqslant 3 \end{cases} \tag{3.22}$$

The comparison of maximum bending stresses obtained using analytical and numerical methods are shown in Fig. 8. The same structures as in Fig. 6 were considered. Both solutions (numerical and analytical) are close, except the region of relatively small deflections. To fix this difference one can add the linear compo-

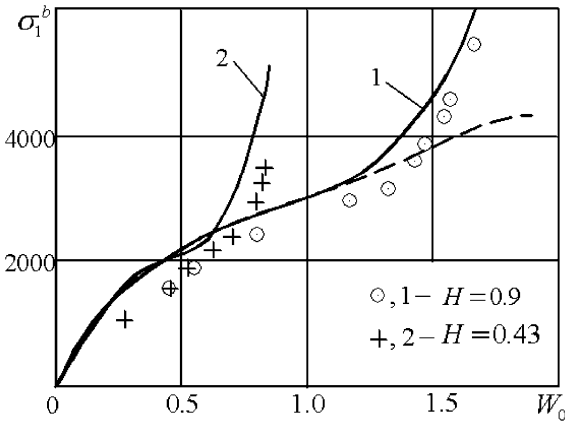

Fig. 8. Bending stresses in clamped spherical shells.

nent of the deflection amplitude according to formula (2.30), corresponding to local deformation of the shell near the load point. However, this formula is valid only for deflection amplitude less than shell thickness and should be corrected for relatively large values of load because of nonlinear shell behavior at this range of deflections.

It is worth to mentioning also that formulas (3.19) and (3.21) are valid only for shallow spherical shells, however they could be applied for estimation of deflections and stresses of deep shells because we have obtained a good agreement of analytical and numerical solutions for this case also (for example, for semi sphere).

4. Conclusion

The asymptotical method, developed in the present paper for the case of deep orthotropic spherical shells under concentrated load, provides simple formulas useful for analyzing nonlinear behavior and stress states of structures, especially for their engineering design. The validation of the analytical solution is based on the main idea of applied asymptotical method as well as on comparison of obtained analytical solution with numerical and experimental results.

References

Ashwell, D.G., 1959. On the large deflection of a spherical shell with an inward point load. In: Proceedings of I.U.T.A.M. Symposium on the Theory of Thin Elastic Shells, Delft, August 1959. North Holland Publication Co., Amsterdam, pp. 43–63.

Bushnell, D., 1967. Bifurcation phenomena in spherical shells under concentrated and ring loads. AIAA Journal 5 (11), 2034–2040.

Evan-Iwanowski, R.M., Cheng, H.S., Loo, T.C., 1962. Experimental investigations of deformations and stability of spherical shells subjected to concentrated load at the apex. In: Proceedings of the Fourth US National Congress of Applied Mechanics, pp. 563–575.

Evkin, A.Yu., Dubichev, A., 1995. Stability of the axisymmetrical equilibrium shape of an orthotropic spherical shell in large bending. Prikladnaya Mekhanika 31 (6), 72–78 (English translation: 1995. International Applied Mechanics 31 (6), 477– 482).

Evkin, A.Yu., Kalamkarov, A.L., 2001a. Asymptotic analysis of large deflection equilibrium states of composite shells of revolution. Part 1. General model and singular perturbation analysis. International Journal of Solids and Structures 38 (50–51), 8961–8974.

Evkin, A.Yu., Kalamkarov, A.L., 2001b. Asymptotic analysis of large deflection equilibrium states of composite shells of revolution. Part 2. Applications and numerical resuts. International Journal of Solids and Structures 38 (50–51), 8975–8987.

Evkin, A.Yu., Korovaitsev, A.V., 1992. Asymptotic analysis of the transcritical axisymmetric state of stress and strain in shells of revolution under strong bending. Izv. Ross. Akad. Nauk. Ser. Makhanika Tverdogo Tela 27 (1), 125–133 (English translation: 1992. Bulletin of the Russian Academy of Science/Mechanics of Solids 27 (1), 121–129).

Fitch, J.R., 1968. The buckling and post-buckling behavior of spherical caps under concentrated load. International Journal of Solids and Structures 4, 421–446.

Mescall, J.F., 1965. Large deflections of spherical shells under concentrated loads. Journal of Applied Mechanics 32 (Transactions of ASME, 87, Series E, December), 935–938.

Penning, F.A., 1966. Experimental buckling modes of clamped shallow shells under concentrated load. Journal of Applied Mechanics 33 (Transactions of ASME, 88, Series E, June 1966) 297–304.

Penning, F.A., Thurston, G.A., 1965. The stability of shallow spherical shells under concentrated load. NASA CR-265, July 1965.

Ranjan, G.V., Steele, C.R., 1977. Large deflection of deep spherical shells under concentrated load. In: Proceedings. AIAA J/ASME 18th Structures. Structural Dynamics and Materials Conference. San Diego, California. Technical paper no 77-411, pp. 269–278.

Reissner, E., 1969. On finite symmetrical deflections of thin shells of revolution. Journal Applied Mechanics 36, 267–270.

Reissner, E., 1972. On finite symmetrical strain in thin shells of revolution. Journal Applied Mechanics 39, 1137–1138.